PCP
PLANT & CELL PHYSIOLOGY

Virus-Induced Silencing of Key Genes Leads to Differential Impact on Withanolide Biosynthesis in the Medicinal Plant, *Withania somnifera*

Aditya Vikram Agarwal[1,2], Deeksha Singh[1,3], Yogeshwar Vikram Dhar[1,3], Rahul Michael[1,3], Parul Gupta[1,4], Deepak Chandra[2] and Prabodh Kumar Trivedi[1,3,*]

[1]Council of Scientific and Industrial Research, National Botanical Research Institute, Rana Pratap Marg, Lucknow 226001, India
[2]Department of Biochemistry, University of Lucknow, Lucknow 226007, India
[3]Academy of Scientific and Innovative Research (AcSIR) Anusandhan Bhawan, 2 Rafi Marg, New Delhi 110001, India
[4]Present address: Botany and Plant Pathology, Oregon State University, 2082-Cordley Hall, Corvallis, OR 97331, USA
*Corresponding author: E-mail, prabodht@nbri.res.in or prabodht@hotmail.com; Fax, +91-522-2205836.
(Received August 7, 2017; Accepted November 13, 2017)

Regular Paper

Withanolides are a collection of naturally occurring, pharmacologically active, secondary metabolites synthesized in the medicinally important plant, *Withania somnifera*. These bioactive molecules are C28-steroidal lactone triterpenoids and their synthesis is proposed to take place via the mevalonate (MVA) and 2-C-methyl-d-erythritol-4-phosphate (MEP) pathways through the sterol pathway using 24-methylene cholesterol as substrate flux. Although the phytochemical profiles as well as pharmaceutical activities of *Withania* extracts have been well studied, limited genomic information and difficult genetic transformation have been a major bottleneck towards understanding the participation of specific genes in withanolide biosynthesis. In this study, we used the *Tobacco rattle virus* (TRV)-mediated virus-induced gene silencing (VIGS) approach to study the participation of key genes from MVA, MEP and triterpenoid biosynthesis for their involvement in withanolide biosynthesis. TRV-infected *W. somnifera* plants displayed unique phenotypic characteristics and differential accumulation of total Chl as well as carotenoid content for each silenced gene suggesting a reduction in overall isoprenoid synthesis. Comprehensive expression analysis of putative genes of withanolide biosynthesis revealed transcriptional modulations conferring the presence of complex regulatory mechanisms leading to withanolide biosynthesis. In addition, silencing of genes exhibited modulated total and specific withanolide accumulation at different levels as compared with control plants. Comparative analysis also suggests a major role for the MVA pathway as compared with the MEP pathway in providing substrate flux for withanolide biosynthesis. These results demonstrate that transcriptional regulation of selected *Withania* genes of the triterpenoid biosynthetic pathway critically affects withanolide biosynthesis, providing new horizons to explore this process further, in planta.

Keywords: Functional genomics • Phenotypic modulations • Transcriptional modulation • Triterpenoid biosynthetic pathway • Virus-induced gene silencing • *Withania somnifera*.

Abbreviations: CP, coat protein; d.p.i., days post-inoculation; IPP, isopentenyl pyrophosphate; MVA, mevalonate; MEP, 2-C-methyl-d-erythritol-4-phosphate; PDS, phytoene desaturase; qRT-PCR, quantitative real-time PCR; TRV, *Tobacco rattle virus*; VIGS, virus-induced gene silencing.

Introduction

Withania somnifera L. Dunal (Solanaceae), commonly known as 'Ashwagandha', 'Asghand' and 'Winter Cherry', is one of the most venerated shrubs of the Indian Ayurvedic system of medicine. Ashwagandha has often been referred to as 'Indian ginseng' and is increasingly becoming a popular adaptogenic herb. Different plant parts (particularly the roots and leaves) of Ashwagandha have been used for a long time in a number of herbal preparations for promoting physiological endurance, overall vitality, strength and general health (Uddin et al. 2012). In the past few decades, there has been a notable surge in the pharmacological-based research in *Withania* demonstrating its anti-tumor, anti-arthritic, anti-aging and neuro-protective properties (Tiwari et al. 2014) in addition to a supportive function in the endocrine, cardiopulmonary and central nervous systems (Mishra et al. 2000), as well as bone health (Khedgikar et al. 2013).

The chemistry of *Withania* species has been extensively studied and the major pharmaceutical activities have been assigned to a group of steroidal lactones known as withanolides. Withanolides are a group of naturally occurring C28-steroidal lactones built on an intact or rearranged ergostane framework, in which C-22 and C-26 are appropriately oxidized to form a six-carbon lactone ring (Mirjalili et al. 2009). Meticulous metabolic profiling of *W. somnifera* identified >40 unique withanolides, along with several glycosylated forms known as sitoindosides, being synthesized and accumulated in different aerial parts, berries and roots of the plant (Chatterjee et al. 2010). In spite of their vast therapeutic potential, commercial exploitation of these specialized molecules has been severely restrained due to their limited availability in purified forms. The concentration of withanolides accumulating in

Plant Cell Physiol. 59(2): 262–274 (2018) doi:10.1093/pcp/pcx179, Advance Access publication on 20 November 2017, available online at www.pcp.oxfordjournals.org
© The Author 2017. Published by Oxford University Press on behalf of Japanese Society of Plant Physiologists.
All rights reserved. For permissions, please email: journals.permissions@oup.com

Downloaded from https://academic.oup.com/pcp/article/59/2/262/4642917 by guest on 20 August 2022

different plant parts of *Withania* has been found to be very low (ranging from 0.001% to 0.5% of DW), with their type and content being modulated by factors such as growth rate, geographical and environmental conditions, chemotype as well as tissue type (Dhar et al. 2013). With very little information available regarding the biogenetic origin and enzymes involved in biosynthetic steps, comprehensive information about the detailed pathway leading to withanolide biosynthesis is still far from understood despite intense research in recent years.

The triterpenoid backbone of withanolides, like other terpenoid compounds, is synthesized from basic isoprene unit precursors [isopentenyl pyrophosphate (IPP) and dimethylallyl pyrophosphate (DMAPP)] (Bhat et al. 2012). Dual autonomous pathways for isoprenoid precursor biosynthesis co-exist in the plant cell including the classical cytosolic mevalonic acid (MVA) pathway and the alternative route, the plastidial methylerythritol phosphate (MEP) pathway (Newman and Chappell 1999). The resultant IPP pool generated through these two independent pathways undergoes various modifications leading to synthesis of a central intermediate C-30 molecule, 24-methylene cholesterol, which has been demonstrated to be the precursor for all withanolides through the radiotracer technique (Glotter 1991). This central molecule further undergoes numerous biochemical transformations including hydroxylation, methylation and glycosylation, leading to the production of an array of diverse withanolides (Dhar et al. 2015). In the past decade, attempts in the area of gene identification and reverse genetic studies including overexpression and down-regulation of expression of putative genes have laid down a strong foundation, encouraging efforts for complete elucidation of withanolide biosynthesis (Singh et al. 2015, Srivastava et al. 2015, Mishra et al. 2016).

Virus-induced gene silencing (VIGS) is a powerful virus-based short interfering RNA-mediated RNA silencing technique which offers an attractive and quick alternative for knocking out expression of a gene for species not amenable to stable genetic transformation (Sha et al. 2014). The technique has been largely adopted for elucidation of biosynthetic pathways of important phytochemicals in medicinal plants including *Papaver somniferum* (Dang and Facchini 2014) and *Catharanthus roseus* (Kumar et al. 2015). Recently, VIGS has been used in *Withania* (Singh et al. 2015) and is becoming a tool of choice for functional genomics in an increasing number of plant species for which gene functions are extremely laborious to analyze by conventional methods.Recently, studies related to identification and expression analysis of genes encoding enzymes for intermediate steps of terpenoid backbone biosynthesis (*WsDXS*, *WsDXR*, *WsHMGR* and *WsFPPS*) have exhibited a pivotal role as key regulatory genes in directing the isoprenoidal flux towards biosynthesis of withanolides (Jadaun et al. 2016). Differential expression of isoforms of these key genes in various tissues and upon elicitor treatments further indicate metabolic channeling of substrates, leading to synthesis of specific withanolides (Agarwal et al. 2017). Involvement of the *WsDWF5-1* isoform in biosynthesis of withaferin A (Gupta et al. 2015) persuaded us to assess the role of this gene family as well as other key regulatory genes.

In this study, we investigated the involvement of five putative genes, i.e. *WsDXS*, *WsDXR*, *WsHMGR*, *WsFPPS* and *WsDWF5*, in the biosynthesis of withanolides by down-regulating their expression in *Withania* using the VIGS approach. Silencing led to significant reduction of total as well as specific withanolides in leaf tissues. Moreover, phenotypic and physiological effects on lines silenced with individual genes as well as perturbations in the expression of other putative withanolide biosynthetic pathway genes were also analyzed.

Results

Silencing of the *PDS* gene in leaves of *Withania*

To test whether the *Tobacco rattle virus* (TRV)-based vector could effectively induce the silencing of endogenous genes in *Withania*, we set out to silence the phytoene desaturase (*WsPDS*) gene, commonly used as a marker due to the resulting easy to score photobleached phenotype, using the TRV:*WsPDS* construct. Syringe infiltration of the TRV:*WsPDS* construct into *Withania* (chemotype NMITLI-135) led to development of bleaching (photobleaching) in the systemic leaves approximately 14 days post-inoculation (d.p.i.) due to *WsPDS* gene silencing (**Fig. 1a**). Most of the treated plants showed strong silencing, where a whole leaf, including the petiole, was photobleached, as compared with control plants. Intermediate phenotypes included scattered sectors of white throughout the plant, and milder ones exhibited photobleaching restricted to the vasculature of leaflets. First, the bleached regions were restricted to the veins of the leaves and later the symptoms extended to most of the leaf tissues. Overall, there was a gradient of silencing phenotypes at the leaflet level (**Fig. 1a**). The overall survival rate of control and treated plants was 100%, indicating that leaf infiltration is suitable for silencing in *Withania*. By comparing the number of plants that showed photobleaching symptoms with the total number of plants that were inoculated with TRV2:*WsPDS*, the calculated gene silencing frequency was recorded as 80%. The effectiveness of gene silencing, in all the plants that showed photobleaching symptoms, was calculated by comparing the number of leaves that showed symptoms with the total number of leaves on the plant, and it was found to be 43%. In order to confirm that the leaf photobleached phenotypes described above correlated with reduced endogenous levels of *WsPDS*, expression of *WsPDS* was analyzed on the newly emerging leaves 30 d.p.i., exhibiting a silencing phenotype compared with control leaves. There was a significant down-regulation of *WsPDS* in photobleached leaf samples, with the percentage silencing efficiency approximately 74% compared with control (**Fig. 1b**). The duration of silencing varied from 8 to 9 weeks from onset, with a few outliers in which silencing continued for up to 3 months.

Silencing of withanolide biosynthesis genes and their affect on growth and development of plant

In order to investigate the role of genes catalyzing production of critical substrates and acting at regulatory steps of withanolide biosynthesis, conserved regions of *WsDXS* (358 bp), *WsDXR*

Downloaded from https://academic.oup.com/pcp/article/59/2/262/4642917 by guest on 20 August 2022

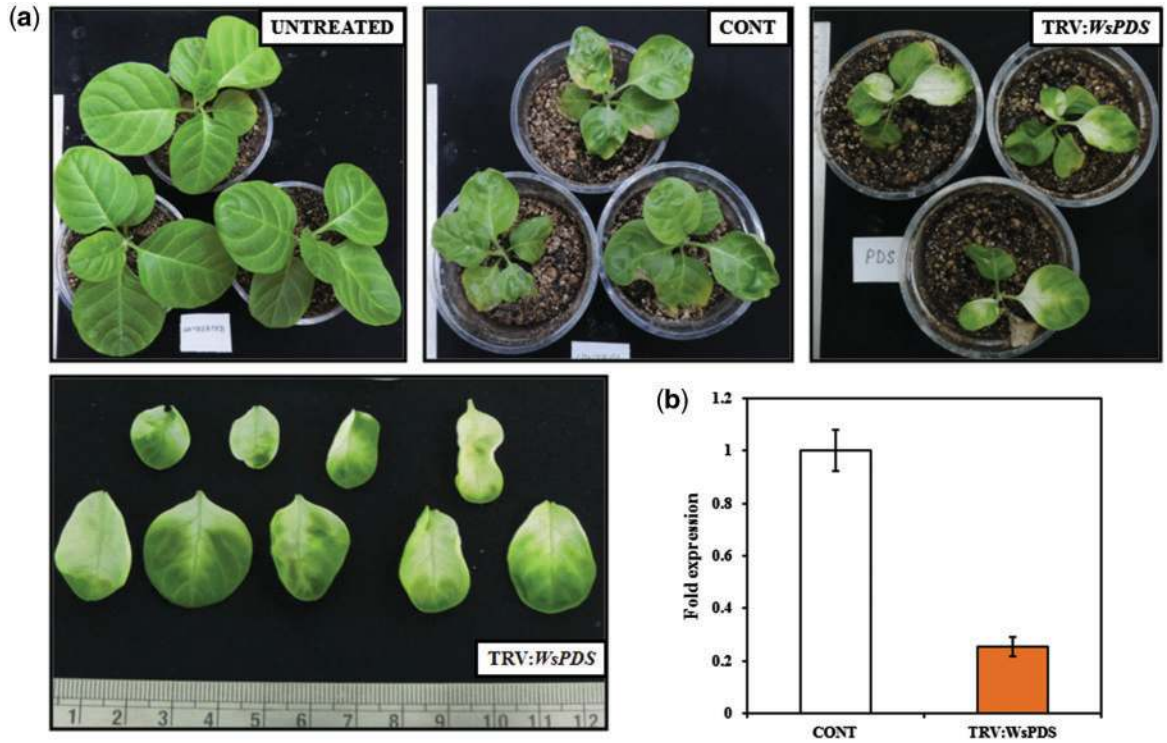

Fig. 1 *Tobacco rattle virus-* (TRV) mediated VIGS silencing of PDS in *Withania somnifera* Phenotype of the wild type (Untreated), empty vector treated (Control) and TRV2:*WsPDS*-treated *W. somnifera* plants at 30 d.p.i. (a). *Withania somnifera* leaves exhibiting a varying degree of photobleached phenotypes in different WsPDS-VIGS leaves at 30 d.p.i. (a, lower panel) and the corresponding mRNA expression levels of PDS analyzed by qRT-PCR (b). The expression levels of PDS transcripts were normalized to actin in comparison with the control. Data are the means ± SE of six biological (n = 6) and three technical replicates. pTRV1, pTRV2 and different fragments of *Withania* genes were used as inserts (~300 bp) for cloning at the multiple cloning site in pTRV2.

(308 bp), *WsHMGR* (307 bp), *WsFPPS* (302 bp) and *WsDWF5-1* (287 bp) were PCR-amplified from leaf cDNA and mobilized into the pTRV2 vector for the development of TRV:*WsDXS*, TRV:*WsDXR*, TRV:*WsHMGR*, TRV:*WsFPPS* and TRV:*WsDWF5-1* constructs, respectively (**Supplementary Fig. S2**). Each construct was able to induce typical viral symptoms of curling and mottling, as well as a unique phenotype along the systemic leaf veins with visible penetrance into non-vascular organs. After 14 d.p.i., typical phenotypic characteristics were visible on the newly developed leaves of treated plants. After an additional 2 weeks, the phenotype could be observed dominating the whole expanded leaf of plants infiltrated with constructs (**Fig. 2a–f**). The silencing effect was detected in all of the treated plants (n >20), indicating a high efficiency of silencing.

Generally, the newly expanded leaves of *WsDXS*-silenced plants displayed yellowish regions, a reduced leaf area and stunted plant height compared with control plants. In the case of *WsDXR*-silenced plants, leaves appeared to be photobleached, having varied albino and green patches distributed on the leaf surface, and the plant height was compromised compared with control plants. Infected leaves in the case of *WsHMGR*-silenced plants appeared to be uniformly yellowish with severe mottling and upward curling at the edges along with reduced leaf area; however, the plant height was not significantly compromised. Ariel parts of *WsFPPS*-silenced lines were the most effected of all the constructs, with severe diminution caused by reduced plant height and leaf area. Silencing of *WsDWF5-1* resulted in an enlargement of aerial parts of the silenced plants, with increased plant height and leaf area, thereby causing a significant overall increase in shoot biomass (**Fig. 3**).

Altered morphology of aerial parts of the silenced plants led us to inspect the underground portion of these plants by studying root length and root biomass. Although no significant changes were recorded, *WsDWF5-1*-silenced lines had visibly increased root length and root biomass, whereas the *WsDXS*-silenced lines were observed to have reduced root length and root biomass (**Fig. 4**).

Silencing of withanolide biosynthesis genes affects Chl and carotenoid content

Altered plant height and pigmentation in the leaves of silenced plants suggested that it was necessary to examine the physiological parameters such as Chl and carotenoid contents. The Chl and carotenoid contents were assessed in the newly emerged leaves, above the infiltrated leaves, that showed the viral phenotype, and was compared with that in the leaves of control plants (**Fig. 5**). The reduction in total Chl content was in accordance with the visible bleaching and yellowing phenotypes of different silenced lines, with the greatest reduction of >80% being observed in the *WsPDS*-silenced plants, followed by an approximately 30% reduction in *WsDXR*-silenced plants. An enhancement in the total Chl content was observed in *WsFPPS*- and *WsDWF5-1*-silenced lines, with an increase of

Downloaded from https://academic.oup.com/pcp/article/59/2/262/4642917 by guest on 20 August 2022

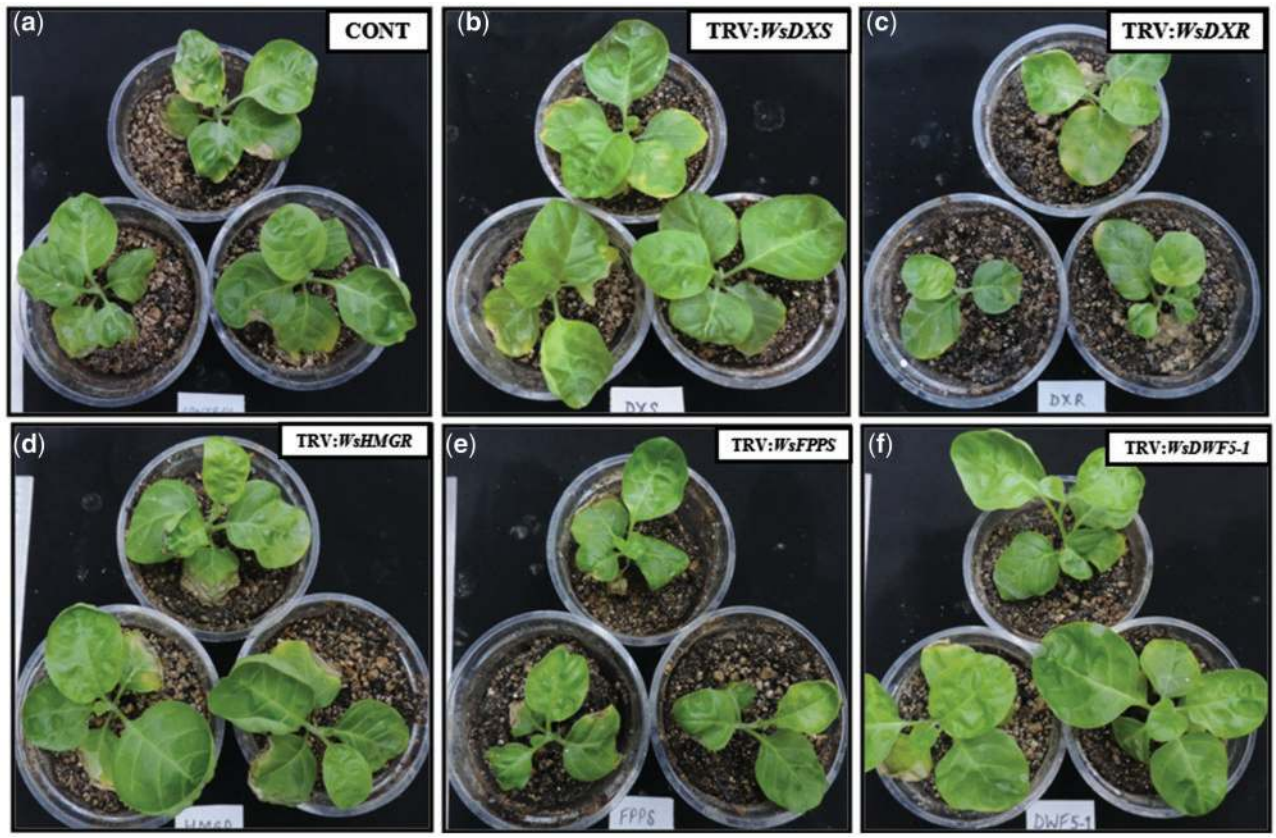

Fig. 2 Representative phenotypes of TRV-silenced plants using different constructs. Typical viral infection phenotype exhibiting slight curling of leaves at 30 d.p.i. in empty vector (Control) lines (a) and different silenced lines of genes putatively involved in withanolide biosynthesis (b–f).

>20% and 40%, respectively. Total Chl content in silenced plants of *WsDXS* and *WsHMGR* did not show significant reduction when compared with control plants. A similar trend of enhancement and reduction in carotenoid content was observed in leaf tissues of plants silenced with different genes of withanolide biosynthesis, with *WsHMGR*-silenced plants showing significantly reduced carotenoid content (**Fig. 5**).

Virus-induced gene silencing reduced the transcript level of withanolide biosynthesis genes

To check the infectivity of TRV, the spread of virus in infiltrated plants was confirmed by semi-quantitative real-time PCR (RT-PCR) using TRV1- and TRV2-specific primers with cDNA prepared from newly emerged leaves. All the control and treated plants showed amplicons corresponding to TRV1 and TRV2 transcripts, providing evidence of a systemic viral infection (**Supplementary Fig. S4**). Amplification of the replicase fragment (**Supplementary Fig. S4a**) and coat protein (CP) fragment (**Supplementary Fig. S4b**) confirmed the occurrence of viral infection in infiltered leaf tissues. RT-PCR performed with TRV2-specific primers spanning the multiple cloning site produced a smaller product size (160 bp) in control plants, corresponding to the distance between primers in the absence of insert, therefore confirming the presence of an empty TRV2 vector; detection of amplicons of greater size in silenced plants confirmed the presence of the transgene in pTRV2 (**Supplementary Fig. S4c**).

To understand the role of selected terpenoid biosynthesis genes in biosynthesis of specific withanolides, rate-limiting and critically positioned genes of the biosynthetic pathway were selected for study. As some of the selected genes are in multiple copies in *Withania* (Agarwal et al. 2017), fragments of sequences used for silencing were chosen, taking into consideration the conserved and complementing nature of multicopy genes as well as the off-target silencing phenomenon. Expression analysis of leaf tissues from infiltrated plants, using specific primers, showed reduced accumulation of transcripts for the different members of the gene families of interest compared with leaf tissues from TRV control plants (**Fig. 6**). Maximum reduction (~80%) in transcript levels was observed in plants infiltrated with the TRV:*WsDWF5-1* construct. Insignificant silencing of *WsDWF5-2* observed in the case of *WsDWF5-1*-silenced VIGS lines reflects the absence of off-target silencing. Although TRV:*WsFPPS*-silenced lines displayed striking phenotypic characteristics, the least effective silencing was recorded for its two isoforms, i.e. 21.6% and 41.4%, showing that WsFPPS is indispensable in terpenoid biosynthesis. On average, the percentage silencing observed in different silenced lines was approximately 50%. (**Supplementary Table S2**).

Silencing of selected withanolide biosynthesis genes modulates expression of other genes of the pathway

Analysis was carried out to study the effect of down-regulation of selected withanolide biosynthesis genes upon expression of

Downloaded from https://academic.oup.com/pcp/article/59/2/262/4642917 by guest on 20 August 2022

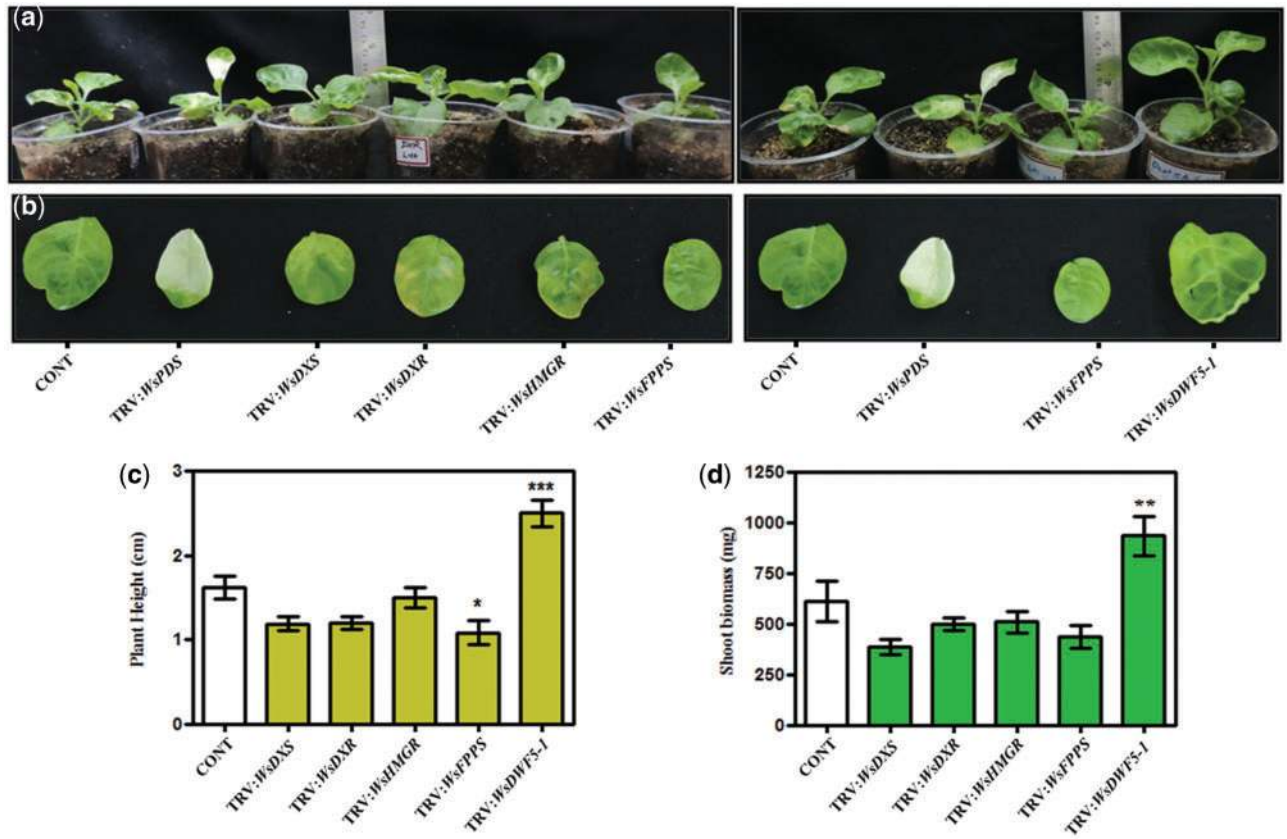

Fig. 3 Plant height and leaf phenotype in different TRV-silenced lines. Down-regulation of *WsDXS*, *WsDXR*, *WsHMGR*, *WsFPPS* and *WsDWF5-1* of *W. somnifera* significantly affects the height (a, c) and shoot biomass (b, d) of the plants. Individual plants are representative of silenced lines of specific genes (a, b). Plant height and shoot biomass data are means ± SE of six biological replicates (n = 6) and three technical replicates.

other genes involved in intermediate steps. To study this, the transcript levels for genes of MVA, MEP (**Fig. 7a**) and downstream (**Fig. 7b**) terpenoid biosynthesis pathways were analyzed in silenced and control samples. It was observed that all the analyzed genes of the terpenoid biosynthesis pathway were modulated in VIGS plants as compared with control, however to different extents.

In general, expression levels of *WsDXS-1*, *WsCDPMEK*, *WsHMGR-1*, *WsHMGR-2*, *WsHMGR-3*, *WsMK*, *WsFPPS-2*, *WsCAS* and *WsDWF5-1* were found to be affected in most of the silenced lines, with significant up- or down-regulation for different constructs, whereas *WsDXS-2*, *WsDXR*, *WsIPI*, *WsFPPS-1*, *WsSQS*, *WsSMO*, *WsFK*, *WsHYD* and *WsDWF-2* had their expression levels modulated in a few or none of the silenced lines (**Fig. 7**). In the case of *WsDXS*-silenced plants, significant modulation in upstream genes of the MVA and MEP pathways was observed; however, expression of downstream genes was not significantly affected. A similar modulation in the expression profile was observed in *WsDXR*-silenced lines along with significant enhancement in *WsHMGR-3* and *WsFPPS* expression. Silencing of *WsHMGR* led to the modulation of expression of the maximum number of genes, including those involved in upstream and downstream intermediate steps, i.e. *WsDXS*, *WsCDPMEK*, *WsMK*, *WsFPPS*, *WsCAS* and *WsDWF5-1*. A mixed response was observed in the case of *WsFPPS*-silenced plants, with *WsCDPMEK*, *WsHMGR* and *WsCAS* being up-regulated, *WsMK* being down-regulated and *WsDXS*, *WsDXR*, *WsSQS* and others being unaffected. In the case of *WsDWF5-1*-silenced lines, there was significant enhancement in expression of specifically the rate-limiting enzymes of terpenoids biosynthesis, i.e. *WsDXS-1*, *WsHMGR-2*, *WsMK*, *WsFPPS2* and *WsCAS*, showing that *WsDWF5-1* is a pivotal gene in regulation of the terpenoid biosynthesis pathway.

Interestingly, significant silencing of all the isoforms of a specific gene was observed when the conserved region was selected for construct preparation. However, silencing was restricted to a particular isoform when the fragment used for silencing was selected from a unique region (**Supplementary Table S2**). There was 69.5% and 50.6% silencing observed in the two isoforms of *WsDXS*, i.e. *WsDXS-1* and *WsDXS-2*, respectively. Similarly, there was marked silencing of the three isoforms of *WsHMGR* as well as two isoforms of *WsFPPS* in the plants silenced by the respective genes. In the case of *WsDWF5*-silenced plants, only one isoform was silenced, whereas the expression of other isoform did not show any significant reduction as the fragment used for silencing was taken from a unique region including the 5′-untranslated region of the isoform sequence (**Supplementary Table S2**).

Down-regulation of withanolide biosynthesis genes modulates specific withanolide content

To investigate the effect of silencing of genes playing a pivotal role in terpenoid backbone biosynthesis towards accumulation

Downloaded from https://academic.oup.com/pcp/article/59/2/262/4642917 by guest on 20 August 2022

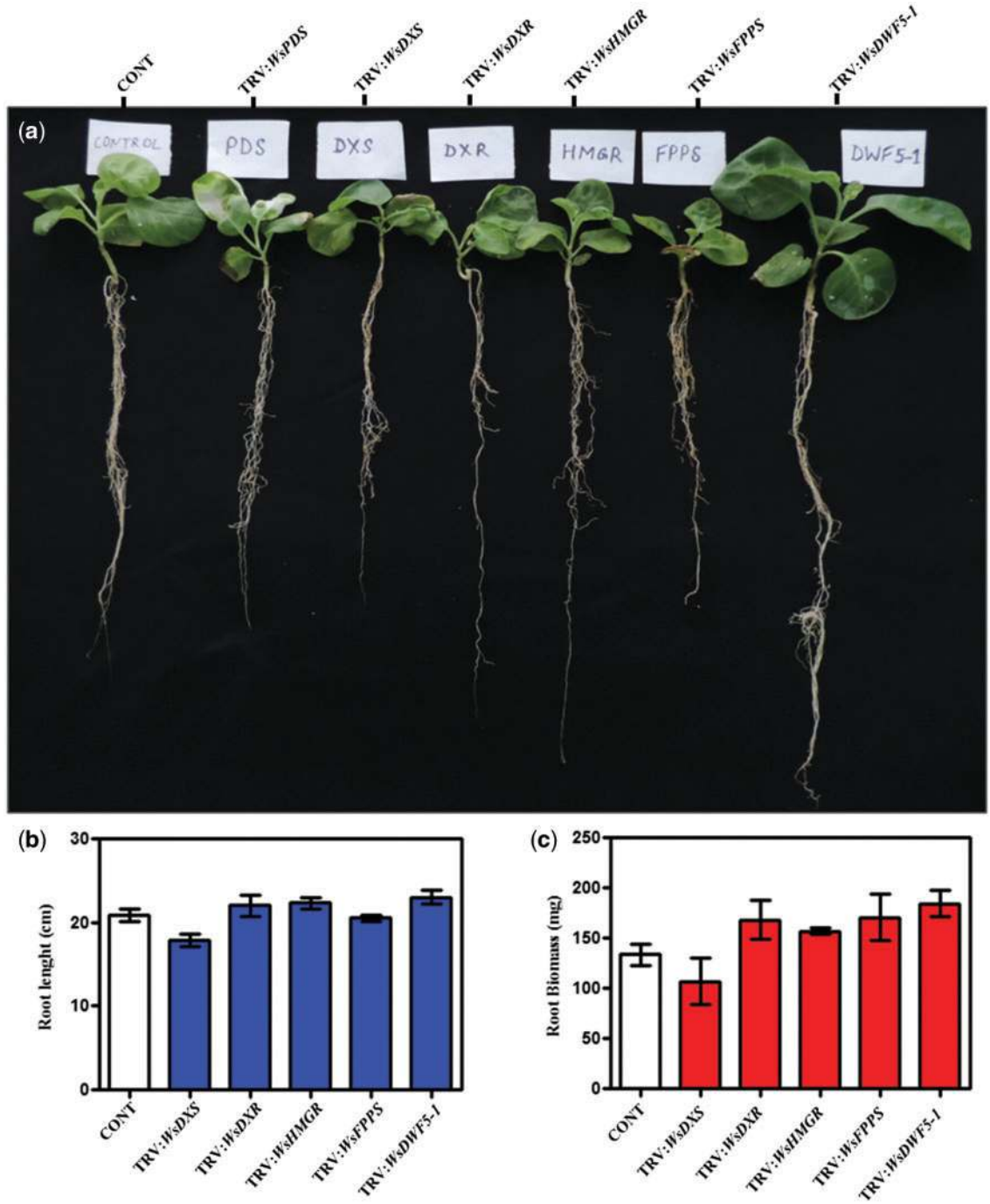

Fig. 4 Root length and root biomass in different TRV-silenced lines. Down-regulation of *WsDXS*, *WsDXR*, *WsHMGR*, *WsFPPS* and *WsDWF5-1* of *W. somnifera* significantly affects the root length (a, b) and root biomass (a, c) of the plants. Individual plants are representative of silenced lines of specific genes (a). Root length and root biomass data are means ± SE of six biological replicate (n = 6) and three technical replicates.

of specific withanolides, we quantified total and specific withanolide contents in leaves of different VIGS-silenced lines of *Withania* at 30 d.p.i. through reverse phase HPLC (**Supplementary Fig. S6**). Quantitative estimation revealed that there is a significant reduction in total withanolide content in all the silenced lines in comparison with the control plants; however, the magnitude of reduction varied for different genes silenced (**Fig. 8a**). The VIGS-treated plants having reduced expression of upstream (MVA and MEP) pathway genes, i.e. *WsDXS*, *WsDXR* or *WsHMGR*, exhibited a slight reduction in total withanolide content; however, plants silenced with genes acting in the downstream pathway, i.e. *WsFPPS* and *WsDWF5-1*, displayed significant reduction of >50% in total withanolide content as compared with control samples.

As withanolide D is known to be the major withanolide in the NMITLI-135 chemotype of *Withania* (Chaurasiya et al. 2009,

Downloaded from https://academic.oup.com/pcp/article/59/2/262/4642917 by guest on 20 August 2022

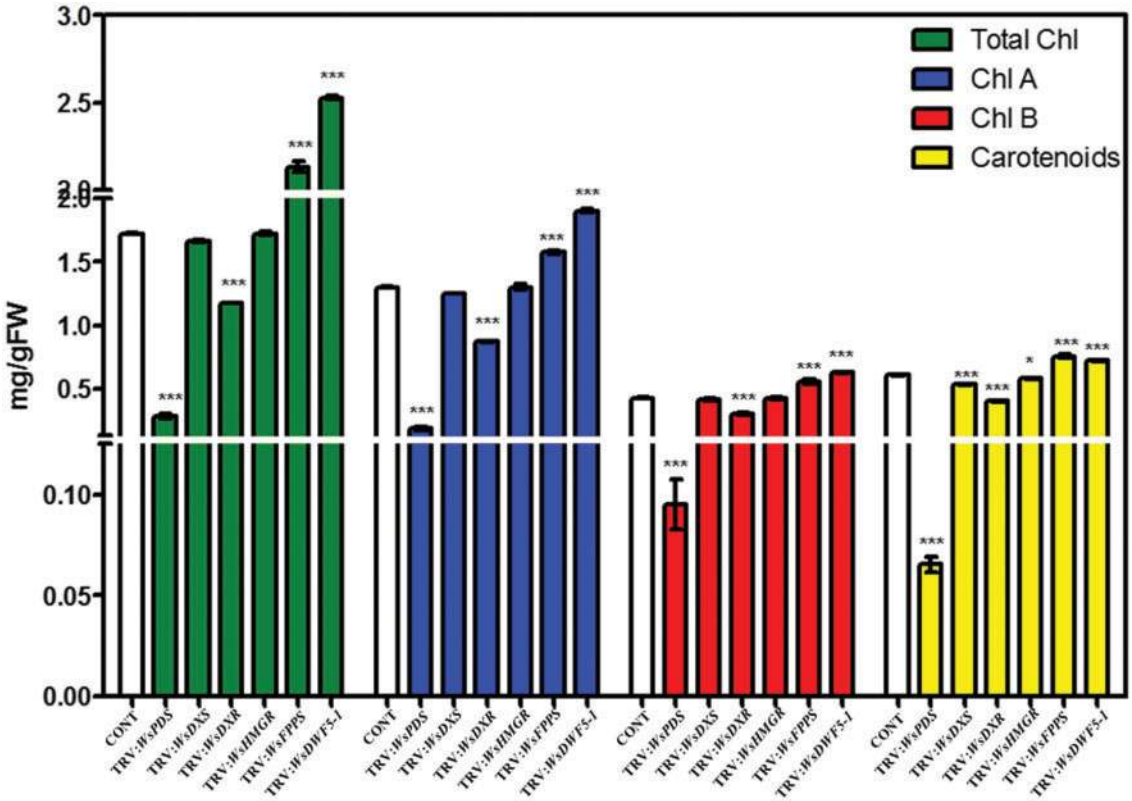

Fig. 5 Chl and carotenoid contents in different TRV-silenced lines. Down-regulation of *WsDXS*, *WsDXR*, *WsHMGR*, *WsFPPS* and *WsDWF5-1* of *W. somnifera* significantly affects the Chl and carotenoid contents of the plants. Chl *a*, Chl *b* and carotenoid content data are means ± SE of six biological replicates (n = 6) and three technical replicates.

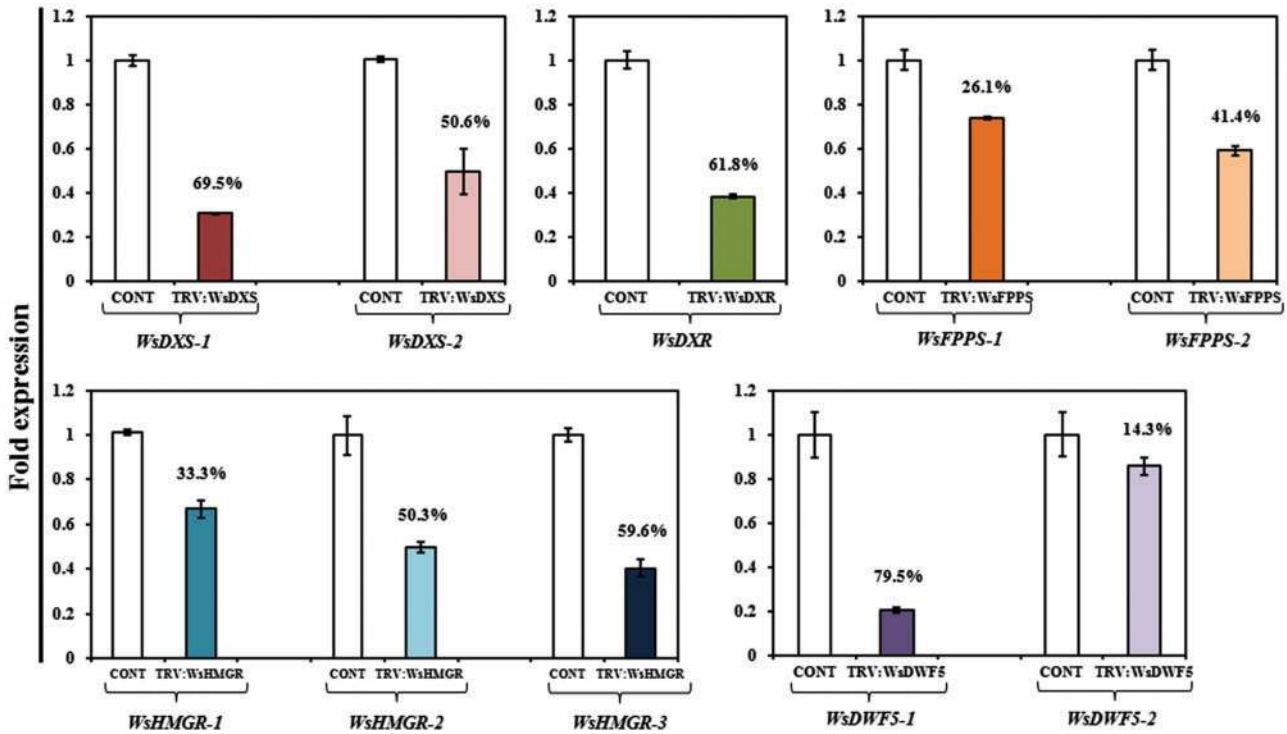

Fig. 6 TRV-mediated silencing affects expression of specific genes and their isoforms. qRT-PCR analysis shows relative expression levels of members of different gene families in systemic leaves of *W. somnifera* plants infiltrated with empty vector (Control) and different VIGS constructs. Actin was used as an internal control. Data are means ± SE of six biological (n = 6) and three technical replicates.

Downloaded from https://academic.oup.com/pcp/article/59/2/262/4642917 by guest on 20 August 2022

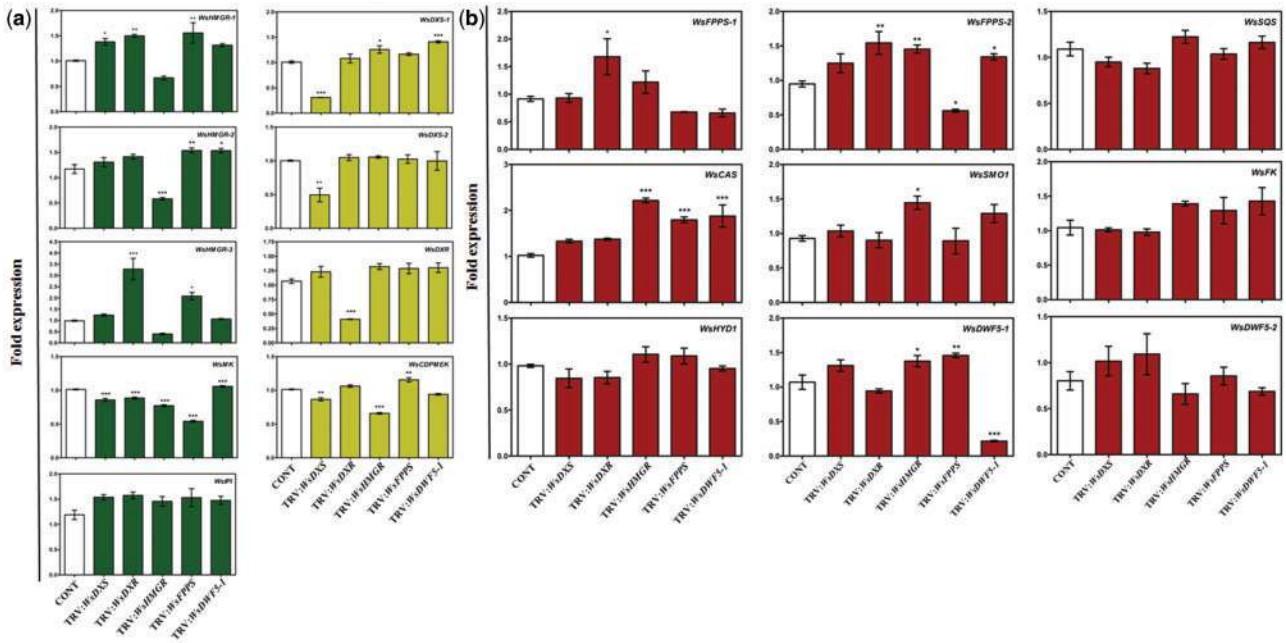

Fig. 7 Differential expression of selected MVA, MEP and Step 2 pathway genes in control and different VIGS lines. qRT-PCR analysis shows relative expression levels of selected MVA, MEP (a) and Step 2 (b) pathway genes in control, *WsDXS*-, *WsDXR*-, *WsHMGR*-, *WsFPPS*- and *WsDWF5-1*-silenced lines in *Withania* leaf. Actin was used as an internal control. Data are means ± SE of six biological (n = 6) and three technical replicates.

Gupta et al. 2015), we set out to estimate the effect of silencing of different genes on its accumulation. It was observed that perturbations in accumulation of withanolide D in different silenced lines roughly matched those for the accumulation of total withanolide content (**Fig. 8**). The VIGS-silenced lines of MEP pathway genes, i.e. *WsDXS* and *WsDXR*, were found to show slight modulation in withanolide D levels (∼10%); however, the *WsHMGR*-silenced lines showed a sharp decline (∼50%) in the content of the molecule. Similarly, there was drastic reduction in the accumulation of withanolide D in samples of *WsFPPS*- and *WsDWF5-1*-silenced plants (∼80%), indicating a dissimilar effect of individual genes of terpenoid backbone biosynthesis on the accumulation of total and specific withanolides in *Withania* leaf tissues (**Fig. 8b**).

Characterization of members of the WsDWF5 family putatively involved in withanolide biosynthesis

As the above results, as well as our previous studies, suggested involvement of a member of the DWF5 gene family in withanolide biosynthesis (Gupta et al. 2015, Agarwal et al. 2017), the structure of both the identified isoforms, i.e. WsDWF5-1 and WsDWF5-2 peptides, was modeled using homology modeling. WsDWF5-1 and WsDWF5-2 have variation in their sequence as well as structure, with the sequence alignment of these two proteins showing 84% identity. The proposed models show a structural organization which contain 18 α-helices and 4 β-strands for WsDWF5-1, whereas 18 α-helices and 2 β-strands were shown for WsDWF5-2. Phylogenetic analysis suggested that WsDWF5-1 is closer to its homologs in *Solanum lycopersicum* and *S. tuberosum*, whereas WsDWF5-2 has more similarity to *Morus notabilis* (**Supplementary Fig. S5a**). Energy minimization results for both proteins reflect that WsDWF5-1 seems more stable than WsDWF5-2 (**Supplementary Fig. S5b**). Although WsDWF5-1 stabilizes at −1.81 kJ mol^{-1} while WsDWF5-2 stabilizes at −2.37 kJ mol^{-1}, it was observed that the stabilized structure of WsDWF5-1 could exist for a longer time, implying greater stability. Expression analysis suggested that although *WsDWF5-1* and *WsDWF-2* were expressed in various tissues of the plant and displayed similar expression patterns, the transcript levels of *WsDWF5-1* were several fold higher than those of *WsDWF5-2* in all the tested tissues (**Supplementary Fig. S5c**), indicating a major catalytic role for WsDWF5-1.

Protein–ligand conformations by automatic docking with chosen ligands have been analyzed using AutoDock tools. The 3D structures of both isoforms were docked with the probable substrate and product. Docking studies of WsDWF5-1 and WsDWF5-2 were carried out using 5-dehydro episterol or 24-methylene cholesterol as ligands (**Supplementary Fig. S5d**). The negative energies indicated a favorable interaction between the proteins and the ligands. The obtained results revealed that the higher interaction energy was observed along with stable bonding, for WsDWF5-1 with 5-dehydroepisterol having a binding energy of −10.06 kcal mol^{-1}. The model revealed that Lys242 is involved in formation of the only H-bond formed between the protein and ligand. A binding energy of −9.89 kcal mol^{-1} was recorded for interaction between WsDWF5-1 and its product, i.e. 24-methylene cholesterol.

For the WsDWF5-2 protein, a binding energy of −9.55 kcal mol^{-1} was recorded upon interaction with 5-dehydroepisterol; however, no formation of a H-bond could be observed. Interaction of WsDWF5-2 with 24-methylene cholesterol

Downloaded from https://academic.oup.com/pcp/article/59/2/262/4642917 by guest on 20 August 2022

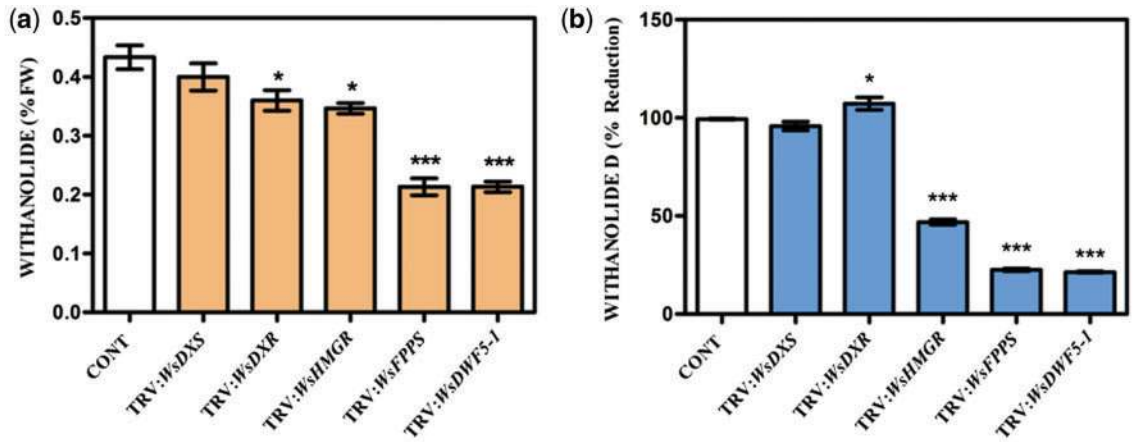

Fig. 8 Relative quantification of total and specific withanolides in control and different VIGS lines. Absolute quantification of total withanolides in leaf tissues of control and silenced lines of various genes of the withanolide biosynthetic pathway (a). Relative quantification of the predominant withanolide (withanolide D) in leaf tissues of control and silenced lines of various genes of the withanolide biosynthetic pathway (b). Data are means ± SE of six biological (n = 6) and three technical replicates.

resulted in a binding energy of −9.81 kcal mol^{-1} by stabilizing the complex through two H-bonds with the same residue ARG405 (**Supplementary Table S3**).

Discussion

Successful metabolic engineering depends upon understanding the enzymes and their regulatory factors involved in intermediate steps of a given pathway. Analysis of gene function in plants has always been a bottleneck towards elucidation of their role in synthesis of specialized molecules (Verpoorte et al. 2000). In the post-genomic era, VIGS has emerged as a powerful reverse genetic tool for the rapid analysis of gene function. In particular, VIGS has gained popularity in plants lacking a high-throughput transformation system (Becker and Lange 2010) and helped in developing information about synthesis of a number of medicinally important molecules (Lakshmi 2012) . Withanolides form an exquisite group of specialized molecules credited with numerous pharmacological properties (Gupta et al. 2015) and found to accumulate in small amounts in the tissues of selected members of the family Solanaceae. Leaf and root tissues of *W. somnifera* have been found to accumulate quantifiable amounts of these biomolecules, thereby being a good model for understanding the synthesis of withanolides (Gupta et al. 2013).

All isoprenoids, precursors for withanolide biosynthesis, are synthesized by the MVA pathway and MEP pathway, and therefore functional characterization of key enzymes catalyzing committed steps of these pathways is indispensable for detailed interpretation of various aspects of specific withanolide accumulation (Gupta et al. 2015). If the amount of plastidic IPP is limiting in the production of isoprenoids, alterations in the IPP level will have an effect on overall isoprenoid levels (Estévez et al. 2001). However, this requirement for IPP can be met by the MVA pathway. Therefore, a balanced participation of these two pathways is essential to provide flux in biosynthesis of specialized molecules. One way to characterize experimentally the rate-limiting steps of a biosynthetic pathway and participation of various MVA or MEP pathway genes is by using reverse genetics to make changes in specific pathways and monitor the corresponding changes in the end-products. Here, a TRV-based VIGS approach has been utilized to determine the function of selected endogenous genes involved in withanolide biosynthesis through participatory involvement of MVA and MEP pathways.

Although different methods have been used for introducing pTRV1/pTRV2 plasmids through *Agrobacterium*-mediated infection, syringe infiltration of seedlings has yielded reliable and consistent silencing of *WsPDS* in previous studies (Singh et al. 2015). The frequency (∼80%) and efficiency (∼43%) of gene silencing obtained through leaf infiltration in our study were comparable with the frequency and efficiency obtained in other Solanaceous plants, confirming an effective and systematic gene silencing (Singh et al. 2015, Singh et al. 2016). Silenced lines of regulatory members of the MVA and MEP pathways generated through the VIGS approach showed phenotypic changes caused by altered growth and development of plants (**Fig. 2**). Plant height, leaf area, root length and root biomass were observed to be significantly affected as compared with the control plants (**Figs. 3, 4**) suggesting perturbations in primary metabolism as well as growth hormone signaling pathways. These results are in agreement with previous reports investigating a reduction in overall isoprenoid synthesis with a reduction in levels of MVA and MEP pathway genes (Jassbi et al. 2008).

It has been shown that sesquiterpenes, triterpenes, cytokinins and brassinosteroids are synthesized via the MVA pathway, while carotenoids, lutein, Chl side-chain, ubiquinone, gibberellins and ABA are synthesized via the MEP pathway (Vranová et al. 2012). Previous studies performed using null mutants of *DXS* have demonstrated modulations in ABA and gibberellin content causing altered phenotype, affirming our VIGS results (Estévez et al. 2001). Similarly, in the case of the *dxr* null mutant, it has been established that the deficiency of gibberellin caused generation of small true leaves and a short petiole in the plant, whereas, reduced levels of ABA caused stomata closing

Downloaded from https://academic.oup.com/pcp/article/59/2/262/4642917 by guest on 20 August 2022

defects. These mutants were also defective for chloroplast development, resulting in an albino phenotype (Xing et al. 2010). In our *WsDXR*-silenced lines, the presence of white patches on leaves, stunted growth of plant and reduced leaf area confirm the previous findings suggesting this gene to be contributing more specifically to the MEP pathway than *DXS* (**Figs. 2c, d, 3a, b**). The T-DNA insertion mutants of *hmgr* have been reported to have a dwarf phenotype, small leaves with yellowing at the edges and reduced root length resulting from a decrease in metabolites downstream of squalene, i.e. sterols and other triterpenoids (Suzuki et al. 2004). These findings corroborate well with our VIGS results showing similar phenotypic characteristics and at the same time a decreased content of withanolides which have a triterpenoid origin (**Figs. 2d, 8a, b**). Conditional knock-down mutants of *FPPS* develop a chlorotic phenotype due to alterations in chloroplast development and a marked alteration in the profile of major cytosolic, mitochondrial and plastidial isoprenoids with a major effect on stigmasterol (Manzano et al. 2016). Reduced overall plant growth in VIGS-silenced plants of *WsFPPS* (**Figs. 3, 4**) reinforces these finding of debilitated and unbalanced sterol accumulation. An unexpected phenotype showing contrasting features from previous studies on *DWF5* mutants was observed in *WsDWF5-1* VIGS-silenced lines. Arabidopsis *dwarf5-2* mutants bearing point mutations in the encoded enzymes are characterized by short height, short internodes, increased number of inflorescences, dark green round leaves and a slow growth rate compared with the wild type (Silvestro et al. 2013). However, VIGS-silenced lines of *WsDWF5-1* displayed enhanced plant height, leaf area and root length (**Figs. 3, 4**). These results indicate that *WsDWF5-1* is positioned at a unique point in withanolide biosynthesis, directing isoprenoid flux specifically towards sterol synthesis. It can be speculated that upon silencing of *WsDWF-1*, the carbon flux may be redirected towards synthesis of brassinolides, a plant hormone regulating various aspects of growth and development, thereby causing enhanced plant growth. Overall it would not be incorrect to say that perturbations in regulatory steps of MVA and MEP pathways cause a complex restructuring of IPP flux, thereby accommodating modulations in diverse primary and secondary metabolites including hormones, steroids, Chl, carotenoids and ubiquinones. The observed phenotypes indicate that terpenoids are stringently controlled and changes in their compositions are rapidly sensed by the plant, in turn activating a series of adaptive responses aimed at coping with the new metabolic scenario.

One important aim in developing TRV VIGS lines for MVA and MEP pathway genes was to obtain a comprehensive understanding about the effect of silencing on expression of different genes of terpenoids biosynthetic pathway. Examination of our quantitative RT-PCR (qRT-PCR) analysis led us to revisit the fact that biosynthesis of terpenoids is tightly regulated and fine-tuned by a complex orchestration of rate-limiting enzymes and distribution of substrate flux in different metabolic channels. Silencing of the genes acting before synthesis of IPP, i.e. *DXS*, *DXR* and *HMGR*, led to major modulations in expression of other genes involved in steps pre-IPP synthesis, revealing a compensatory mechanism to maintain the IPP pool inside the cell (**Fig. 7a**). Moreover, modulation of expression of the maximum number of genes involved in terpenoid backbone biosynthesis in *WsHMGR*-silenced lines supports the view that WsHMGR is one of the key regulatory enzymes of terpenoid biosynthesis. Expression analysis of various genes in *DWF5-1*-silenced lines present new evidence for DWF5-1 playing a critical role in regulation of terpenoid biosynthesis through significant modulation in expression of all the rate-limiting enzymes of the pathway (**Fig. 7**).

It seems evident from the results that all the genes silenced in this study play an indispensable role in withanolide production. A small modulation in accumulation of withanolide D as well as total withanolide content was observed in leaf tissues of *WsDXS*- and *WsDXR*-silenced plants (**Fig. 8**). These results seem to be logical as both these genes catalyze initial steps of the MEP pathway providing flux for production of numerous terpene-derived products, and therefore show a direct although weak relationship with withanolide biosynthesis. A similar observation was noted in the case of *WsHMGR*-silenced lines showing marginal reduction in total withanolide content (**Fig. 8a**); however, the reduction in withanolide D was found to be more prominent in this case as compared with MEP pathway genes (**Fig. 8b**). As HMGR has been repeatedly reported to be a pivotal enzyme in sterol biosynthesis, reduced levels of specific withanolides suggests that *WsHMGR* and the MVA pathway might play an important role in biosynthesis of withanolides. Marked reduction in levels of total withanolides as well as withanolide D observed in leaf tissues of *Withania* plants silenced with *WsFPPS* and *WsDWF5-1* are a proof-of-concept substantiating our previous reports (Gupta et al. 2011, Gupta et al. 2015) that WsFPPS plays an indispensable role in withanogenesis and all withanolides are synthesized from a sole precursor, i.e. 24-methylene cholesterol. WsDWF5-1, which is involved in the last steps of the post-squalene sterol biosynthetic segment, is considered one of the highly conserved enzymes among plants, animals and fungi. As 24-methlene cholesterol is the direct product of catalysis of DWF5 (Gupta et al., 2015), it is acceptable that down-regulation of *DWF5-1* in *Withania* leads to reduced levels of the corresponding product and therefore ultimate reduction of total and specific withanolides, which is reflected in our results.

The observed critical role of members of the WsDWF5 gene family (Gupta et al. 2015, Agarwal et al, 2017) evoked us to determine the catalytic behavior of the two characterized members of the DWF5 family so as to get a closer look at their role in withanogenesis. The structural model of these two members is not available in any database. Differences in secondary structure indicate that the two enzymes cater for a different set of substrates or differential specificity towards individual intermediates of the withanolide biosynthetic pathway. Greater stability of WsDWF5-1 in comparison with WsDWF5-2 through energy minimization implies that WsDWF5-1 must be playing a major role in catalyzing substrates towards withanolide production. Expression analysis also shows a predominant role for the WsDWF5-1 isoform in catalysis of the representative step of withanolide biosynthesis. Protein–ligand conformations using automatic docking tools suggest that 5-dehydro episterol is the preferred substrate over

Downloaded from https://academic.oup.com/pcp/article/59/2/262/4642917 by guest on 20 August 2022

24-methylene cholesterol for both of the family members; however, they show a different affinity for the same substrate. It can be rightly said that comprehensive expression analysis of putative genes of withanolide biosynthesis revealed transcriptional modulations conferring the presence of a network of regulatory mechanisms governing the process.

In conclusion, we demonstrate the involvement of *WsDXS*, *WsDXR*, *WsHMGR*, *WsFPPS* and *WsDWF5-1* genes in biosynthesis of specific withanolides in leaf tissues of *Withania* using the VIGS approach. The decreased transcription levels of corresponding genes in different *Withania* silenced lines reflect their reduced enzymatic activity in vivo, thereby stepping down production of critical intermediates. This deficit of intermediates very likely triggers a multilevel compensatory response ensuing perturbations in the expression of other pathway genes. Moreover, development of unique phenotypes in VIGS-silenced lines confirms involvement of these genes in primary metabolism affecting the growth and development of the plant. These findings contribute to our overall knowledge about withanogenesis and its regulation in *Withania* leaf tissues, and at the same time provide new opportunities to uncover the relationship between putative biosynthesis genes and withanolide accumulation in different chemotypes and tissues. Finally, successful implementation of VIGS for elucidation of withanolide biosynthesis in *Withania* can steer the attempts towards exploring other rare natural products.

Materials and Methods

Plant material, plasmids and bacterial strains

Withania somnifera chemotype (NMITLI-135) was developed under the CSIR-New Millennium Indian Technology Leadership Initiative (CSIR-NMITLI) Program and maintained at an experimental plot in the institute under standard cultivation conditions. Seeds were germinated in plastic pots containing Soilrit. Seedlings were transplanted into individual plastic cups at the two-leaf stage. After a week, when plants reached the four-leaf stage, agro-infiltration was carried out. After infiltration, plants were kept in the dark overnight and then placed in a glass house under controlled growth conditions (22°C and 16 h day/8 h night cycle). Newly emerged leaves from infiltrated plants showing typical viral infection symptoms were collected at 30 d.p.i. and stored at − 70°C for further analysis. All constructs prepared for the study were initially cloned in pTZ57R/T plasmid (Fermentas). For VIGS assay, the pTRV1 and pTRV2 vectors (Liu et al. 2002) obtained from TAIR (www.arabidopsis.org) were used in this study. Bacterial strains employed in the study are *Escherichia coli* DH5α (for cloning) and *Agrobacterium tumefaciens* LBA4404 (for VIGS assay).

Gene cloning and construct preparation

Gene fragments (~300 bp) (**Supplementary Fig. S2**) were amplified, for a selected set of genes involved in withanolide biosynthesis, using cDNA as a template and gene-specific primers. Fragments were cloned into the pTRV2 vector to form the pTRV2:*GOI* construct. Sequences of oligonucleotides used for cDNA amplification and construct preparation are given in **Supplementary Table S1**. For silencing of *WsPDS*, the TRV2:*WsPDS* construct prepared by Singh et al. (2015) was used in this study. Each construct was sequenced to ensure error-free cloning using a capillary automated sequencer (ABI 3730 DNA Analyzer) as per the manufacturer's instructions.

Agrobacterium infiltration/VIGS assay

For VIGS assay (**Supplementary Fig. S3**), pTRV1- and pTRV2-derived constructs were transformed into the LBA4404 strain of *A. tumefaciens* through electroporation. Positive transformants were selected through colony PCR and grown on YEB agar medium (50 mg ml^{-1} kanamycin, 250 mg ml^{-1} streptomycin and 25 mg ml^{-1} rifampicin). Briefly, 2 d before infiltration, 5 ml primary cultures of *Agrobacterium* strains were inoculated from single positive colonies on plates and grown for 16 h at 28 °C. A secondary culture (50 ml) was inoculated from the primary culture and grown overnight to obtain an OD_{600} of 0.6. The cultures were centrifuged at 3,000×*g* for 10 min at 4 °C and cells were resuspended in infiltration medium (10 mM MES, 200 μM acetosyringone, 10 mM $MgCl_2$) to obtain an OD_{600} of 1.2 and incubated at 28 °C for 3–4 h. pTRV1 was co-infiltrated with pTRV2, pTRV2:*WsPDS* or pTRV2:*GOI* in a 1 : 1 ratio on the abaxial surface of leaves in four-leaf-stage *Withania* plants. Infiltration of TRV1::TRV2 in the plants served as the empty vector control (EV). After infiltration, plants were kept in the dark overnight and then placed in a glass house under controlled growth conditions (22 ± 2°C and 16 h day/8 h night cycle). Newly emerged leaves from infiltrated plants showing typical viral infection symptoms were collected at 30 d.p.i. and stored at − 80 °C for further analysis. At least 20 independent plants were used for the infiltration experiment for each construct, and six independent infiltrated plants were used for further analysis.

Confirmation of transgenes and qRT-PCR-based expression analysis

Total RNA was extracted from newly emerged leaves of plants using an RNA isolation kit (Sigma-Aldrich) and treated with RNase-free DNase I (Ambion). First-strand cDNA was synthesized using 5 μg of total RNA with an oligo(dT) primer (Fermentas). To detect the presence of TRV in the collected samples, RNA1 and RNA2 of TRV were amplified by two pairs of vector-specific primers amplifying replicase and CP genes, respectively (**Supplementary Table S1**). To determine relative levels of expression in silenced lines, qRT-PCR was performed using primers that annealed outside the region targeted for silencing, to ensure that only the endogenous gene would be tested. Quantitative expression of genes in different VIGS-silenced lines was analyzed using the qRT-PCR Detection System and Fast SYBR Green PCR Master Mix (ABI 7500, Applied Biosystems). For each primer set, a control reaction was also included having no template. The actin gene from *W. somnifera* was used as an internal control to estimate the relative transcript level of the genes analyzed. Data from qRT-PCR amplification were analyzed using the comparative Ct ($2^{-\Delta\Delta ct}$) method (Agarwal et al., 2017). Fold change in expression was calculated as $2^{-\Delta\Delta ct}$ using ΔCt values. All the experiments were repeated using six biological replicates and three technical replicates. Gene-specific oligonucleotides used for qRT-PCR analysis are provided in **Supplementary Table S1**.

Analysis of phenotypic variation

Phenotypic variation in treated and control plants was carefully observed and consistently monitored. Shoot height, shoot biomass, root length and root biomass were recorded at 30 d.p.i. for at least 20 independent plants for each construct, out of which six independent plants were used for further analysis.

Chl and carotenoid estimation

For Chl analysis, 100 mg of collected samples were crushed in 5 ml (80%, v/v) of chilled acetone (Arnon 1949). Homogenized leaf tissues were centrifuged at 7,800×*g* for 10 min at 4 °C and the supernatant was collected and kept in the dark. Absorbance of clear supernatant was recorded at 663, 645, 510 and 480 nm. The amounts of total Chl, Chl *a* and Chl *b* were calculated in (mg g^{-1} FW) using the formula of Maclachlan and Zalik (1963). The formula given by Dexbury and Yentch (1956) was used to calculate carotenoid content in mg g^{-1} FW

Phytochemical analysis

Extraction and analysis of withanolides from pooled tissues (1 g of fresh tissue) of different VIGS-silenced lines was carried out essentially according to Chaurasiya et al. (2009). Briefly, the chloroform fractions were pooled, concentrated to a dry powder, dissolved in HPLC grade methanol, filtered (Millex GV; 13 mm, 0.22 μm filters) and subjected to reverse phase HPLC. The relative content of withanolide D was assessed using HPLC-PDA connected to a Shimadzu LC-10A system comprising an LC-10AT dual-pump system, an

Downloaded from https://academic.oup.com/pcp/article/59/2/262/4642917 by guest on 20 August 2022

SPD-10A PDA detector (operated at 227 nm) and a Rheodyne injection valve with a 20 µl sample loop. Compounds were separated on an RP-C18 column (Merck) (4.6 mm × 250 mm, 5 µm pore size). Total withanolide content was measured as µg mg^{-1} of withanolides accumulating in leaf tissues of different silenced lines to assess the effects on withanogenesis.

Data analysis

A completely randomized design was used for all treatments. The values are the mean ± SE for samples in each group. Statistical analysis was performed by one-way analysis of variance (ANOVA) followed by Dunnett's post-test, using GraphPad Prism 5. Asterisks in the figures indicate significance levels with $^{*}P < 0.05$; $^{**}P < 0.01$; $^{***}P < 0.001$.

Supplementary data

Supplementary data are available at PCP online.

Funding

This work was supported by the Council of Scientific and Industrial Research, New Delhi, Govt. of India [under the NMITLI scheme]; the Indian Council of Medical Research [senior research fellowship to A.V.A]; University Grants Commission [junior and senior research fellowship to D.S.]; the Council of Scientific and Industrial Research [fellowships to P.G. and Y.V.D]; and Department of Science & Technology [junior and senior research fellowship to R.M.].

Acknowledgments

The authors acknowledge Dr. N.S. Sangwan and Dr. R.S. Sangwan (CSIR-CIMAP) for developing and sharing *Withania* chemotypes under the NMITLI scheme, Dr. O.P. Sihdu, and Annie Agarwal (CSIR-NBRI) for help with HPLC, and Dr. D. A. Nagegowda, Principal Scientist (CSIR-CIMAP) for sharing the TRV:*WsPDS* construct as a kind gift. P.K.T. and D.C. designed the project strategy; A.V.A. and D.S. performed the virus-induced gene silencing, expression analysis, phenotype analysis and metabolite analysis; Y.V.D. and A.V.A. performed the in silico analysis, A.V.A. drafted and wrote the manuscript with assistance from R.M., P.G., D.C. and P.K.T.

Disclosures

The authors have no conflicts of interest to declare.

References

Agarwal, A.V., Gupta, P., Singh, D., Dhar, Y.V., Chandra, D. and Trivedi, P.K. (2017) Comprehensive assessment of the genes involved in withanolide biosynthesis from *Withania somnifera*: chemotype-specific and elicitor-responsive expression. *Funct. Integr. Genomics*: 1–14.

Arnon, D.I. (1949) Copper enzymes in isolated chloroplasts. Polyphenoloxidase in *Beta vulgaris*. *Plant Physiol.* 24: 1.

Becker, A. and Lange, M. (2010) VIGS—genomics goes functional. *Trends Plant Sci.* 15: 1–4.

Bhat, W.W., Lattoo, S.K., Razdan, S., Dhar, N., Rana, S., Dhar, R.S., et al. (2012) Molecular cloning, bacterial expression and promoter analysis of squalene synthase from *Withania somnifera* (L.) Dunal. *Gene* 499: 25–36.

Chatterjee, S., Srivastava, S., Khalid, A., Singh, N., Sangwan, R.S., Sidhu, O.P., et al. (2010) Comprehensive metabolic fingerprinting of *Withania somnifera* leaf and root extracts. *Phytochemistry* 71: 1085–1094.

Chaurasiya, N.D., Sangwan, R.S., Misra, L.N., Tuli, R. and Sangwan, N.S. (2009) Metabolic clustering of a core collection of Indian ginseng *Withania somnifera* Dunal through DNA, isoenzyme, polypeptide and withanolide profile diversity. *Fitoterapia* 80: 496–505.

Dang, T.-T.T. and Facchini, P.J. (2014) Cloning and characterization of canadine synthase involved in noscapine biosynthesis in opium poppy. *FEBS Lett.* 588: 198–204.

Dexbury, A. and Yentch, C. (1956) Plankton pigment monograph. *J. Mater. Res.* 15: 93–101.

Dhar, N., Rana, S., Bhat, W.W., Razdan, S., Pandith, S.A., Khan, S., et al. (2013) Dynamics of withanolide biosynthesis in relation to temporal expression pattern of metabolic genes in *Withania somnifera* (L.) Dunal: a comparative study in two morpho-chemovariants. *Mol. Biol. Rep.*. 40: 7007–7016.

Dhar, N., Razdan, S., Rana, S., Bhat, W.W., Vishwakarma, R. and Lattoo, S.K. (2015) A decade of molecular understanding of withanolide biosynthesis and in vitro studies in *Withania somnifera* (L.) Dunal: prospects and perspectives for pathway engineering. *Front. Plant Sci.* 6: 1031.

Estévez, J.M., Cantero, A., Reindl, A., Reichler, S. and León, P. (2001) 1-Deoxy-D-xylulose-5-phosphate synthase, a limiting enzyme for plastidic isoprenoid biosynthesis in plants. *J. Biol. Chem.* 276: 22901–22909.

Glotter, E. (1991) Withanolides and related ergostane-type steroids. *Nat. Prod. Rep.* 8: 415–440.

Gupta, P., Goel, R., Agarwal, A.V., Asif, M.H., Sangwan, N.S., Sangwan, R.S., et al. (2015) Comparative transcriptome analysis of different chemotypes elucidates withanolide biosynthesis pathway from medicinal plant *Withania somnifera*. *Sci. Rep.* 5: 18611.

Gupta, P., Goel, R., Pathak, S., Srivastava, A., Singh, S.P. and Sangwan, R.S. (2013) De novo assembly, functional annotation and comparative analysis of *Withania somnifera* leaf and root transcriptomes to identify putative genes involved in the withanolides biosynthesis. *PLoS One* 8: e62714.

Jadaun, J.S., Sangwan, N.S., Narnoliya, L.K., Singh, N., Bansal, S., Mishra, B., et al. (2016) Over-expression of DXS gene enhances terpenoidal secondary metabolite accumulation in rose-scented geranium and *Withania somnifera*: active involvement of plastid isoprenogenic pathway in their biosynthesis. *Physiol. Plant.* 159: 381–400.

Jassbi, A.R., Gase, K., Hettenhausen, C., Schmidt, A. and Baldwin, I.T. (2008) Silencing geranylgeranyl diphosphate synthase in *Nicotiana attenuata* dramatically impairs resistance to tobacco hornworm. *Plant Physiol.* 146: 974–986.

Khedgikar, V., Kushwaha, P., Gautam, J., Verma, A., Changkija, B., Kumar, A., et al. (2013) Withaferin A: a proteasomal inhibitor promotes healing after injury and exerts anabolic effect on osteoporotic bone. *Cell Death Dis.* 4: e778.

Kumar, K., Kumar, S.R., Dwivedi, V., Rai, A., Shukla, A.K., Shanker, K., et al. (2015) Precursor feeding studies and molecular characterization of geraniol synthase establish the limiting role of geraniol in monoterpene indole alkaloid biosynthesis in *Catharanthus roseus* leaves. *Plant Sci.* 239: 56–66.

Liu, Y., Schiff, M. and Dinesh-Kumar, S. (2002) Virus-induced gene silencing in tomato. *Plant J.* 31: 777–786.

Maclachlan, S. and Zalik, S. (1963) Plastid structure, chlorophyll concentration, and free amino acid composition of a chlorophyll mutant of barley. *Can. J. Bot.* 41: 1053–1062.

Manzano, D., Andrade, P., Caudepón, D., Altabella, T., Arró, M. and Ferrer, A. (2016) Suppressing farnesyl diphosphate synthase alters chloroplast

Downloaded from https://academic.oup.com/pcp/article/59/2/262/4642917 by guest on 20 August 2022

development and triggers sterol-dependent induction of JA and Fe-related responses. *Plant Physiol*. 172: 93–117.

Mirjalili, M.H., Moyano, E., Bonfill, M., Cusido, R.M. and Palazón, J. (2009) Steroidal lactones from *Withania somnifera*, an ancient plant for novel medicine. *Molecules* 14: 2373–2393.

Mishra, L.-C., Singh, B.B. and Dagenais, S. (2000) Scientific basis for the therapeutic use of *Withania somnifera* (ashwagandha): a review. *Alt. Med. Rev*. 5: 334–346.

Mishra, S., Bansal, S., Mishra, B., Sangwan, R.S., Jadaun, J.S. and Sangwan, N.S. (2016) RNAi and homologous over-expression based functional approaches reveal triterpenoid synthase gene-cycloartenol synthase is involved in downstream withanolide biosynthesis in *Withania somnifera*. *PLoS One* 11: e0149691.

Newman, J.D. and Chappell, J. (1999) Isoprenoid biosynthesis in plants: carbon partitioning within the cytoplasmic pathway. *Crit. Rev. Biochem. Mol. Biol.* 34: 95–106.

Sha, A., Zhao, J., Yin, K., Tang, Y., Wang, Y., Wei, X., et al. (2014) Virus-based microRNA silencing in plants. *Plant Physiol.* 164: 36–47.

Silvestro, D., Andersen, T.G., Schaller, H. and Jensen, P.E. (2013) Plant sterol metabolism. Δ7-Sterol-C 5-desaturase (STE1/DWARF7), Δ5, 7-sterol-Δ7-reductase (DWARF5) and Δ24-sterol-Δ24-reductase (DIMINUTO/DWARF1) show multiple subcellular localizations in *Arabidopsis thaliana* (Heynh) L. *PLoS One* 8: e56429.

Singh, A.K., Dwivedi, V., Rai, A., Pal, S., Reddy, S.G.E., Rao, D.K.V., et al. (2015) Virus-induced gene silencing of *Withania somnifera* squalene synthase negatively regulates sterol and defence-related genes resulting in reduced withanolides and biotic stress tolerance. *Plant Biotechnol. J.* 13: 1287–1299.

Singh, G., Tiwari, M., Singh, S.P., Singh, S., Trivedi, P.K. and Misra, P. (2016) Silencing of sterol glycosyltransferases modulates the withanolide biosynthesis and leads to compromised basal immunity of *Withania somnifera*. *Sci. Rep.* 6: 25562.

Srivastava, S., Sangwan, R.S., Tripathi, S., Mishra, B., Narnoliya, L., Misra, L., et al. (2015) Light and auxin responsive cytochrome P450s from *Withania somnifera* Dunal: cloning, expression and molecular modelling of two pairs of homologue genes with differential regulation. *Protoplasma* 252: 1421–1437.

Suzuki, M., Kamide, Y., Nagata, N., Seki, H., Ohyama, K., Kato, H., et al. (2004) Loss of function of 3-hydroxy-3-methylglutaryl coenzyme A reductase 1 (HMG1) in Arabidopsis leads to dwarfing, early senescence and male sterility, and reduced sterol levels. *Plant J.* 37 : 750–761.

Tiwari, R., Chakraborty, S., Saminathan, M., Dhama, K. and Singh, S.V. (2014) Ashwagandha (*Withania somnifera*): role in safeguarding health, immunomodulatory effects, combating infections and therapeutic applications: a review. *J. Biol. Sci.* 14: 77.

Uddin, Q., Samiulla, L., Singh, V. and Jamil, S. (2012) Phytochemical and pharmacological profile of *Withania somnifera* Dunal: a review. *J. Appl. Pharmaceut. Sci*. 2: 170–175.

Verpoorte, R., van der Heijden, R. and Memelink, J. (2000) Engineering the plant cell factory for secondary metabolite production. *Transgenic Res.* 9: 323–343.

Vranová, E., Coman, D. and Gruissem, W. (2012) Structure and dynamics of the isoprenoid pathway network. *Mol. Plant* 5: 318–333.

Xing, S., Miao, J., Li, S., Qin, G., Tang, S., Li, H., et al. (2010) Disruption of the 1-deoxy-D-xylulose-5-phosphate reductoisomerase (DXR) gene results in albino, dwarf and defects in trichome initiation and stomata closure in *Arabidopsis*. *Cell Res.* 20: 688–700.

Downloaded from https://academic.oup.com/pcp/article/59/2/262/4642917 by guest on 20 August 2022